

Article

Multi-Scale Observations of Atmosphere Environment and Aerosol Properties over North China during APEC Meeting Periods

Xi Wei^{1,2}, Xingfa Gu¹, Hao Chen^{1,*}, Tianhai Cheng^{1,*}, Ying Wang¹, Hong Guo¹, Fangwen Bao^{1,2} and Kunsheng Xiang^{1,2}

Received: 30 September 2015; Accepted: 25 December 2015; Published: 31 December 2015

Academic Editor: Robert W. Talbot

¹ State Key Laboratory of Remote Sensing Science, Institute of Remote Sensing and Digital Earth of Chinese Academy of Sciences, Beijing 100101, China; weixi@radi.ac.cn (X.W.); xfgu@radi.ac.cn (X.G.); wangying@radi.ac.cn (Y.W.); guohong@radi.ac.cn (H.G.); baofw@radi.ac.cn (F.B.); xiangks@radi.ac.cn (K.X.)

² University of Chinese Academy of Sciences, Beijing 100049, China

* Correspondence: chen hao@radi.ac.cn (H.C.); chength@radi.ac.cn (T.C.); Tel./Fax: +86-64-839-949

Abstract: This paper reveals a study on air pollution process over North China, applying remote sensing technology, using satellite observation and *in situ* measurements during the twenty-first Asia-Pacific Economic Cooperation (APEC) meeting, which was held in Beijing between 6 and 12 November when the clear weather was called “APEC-Blue”. In the meantime, pollutants concentrations including PM_{2.5} and PM₁₀ in Beijing were lower than 100 µg/m³ owing to the effective government measures and policies, as well as meteorological conditions. High aerosol loading (AOD > 1) was observed over south of Beijing and vertical observations showed that the pollutants were prominent near the land surface. Different from the meeting period, high pollutants concentrations with explosive growth (the values of PM_{2.5} and PM₁₀ peaking at 291 µg/m³ and 360 µg/m³ respectively) appeared over Beijing after the meeting period, accompanied by strong temperature inversion and high Relative Humidity (RH) values. The pollution particles transferred from Beijing area to south part of North China. Otherwise, fine-mode particles with strong absorption characteristic (UVAI > 1.5, AOD > 1) covered the Beijing sky in the meantime, indicating the existence of black carbon aerosols.

Keywords: APEC; atmosphere environment; aerosol; optical properties; meteorological condition; satellite data

1. Introduction

China has made an extremely rapid economic growth in recent decades, which has led to an increase of resource consumption, environment deterioration and relevant health problems. As the nation’s capital, the air condition of Beijing is characterized by the heavy anthropogenic emissions throughout the year. Between 6 and 12 November, the twenty-first Asia-Pacific Economic Cooperation (APEC) convention was held in Beijing. For the sake of guaranteeing the smooth convening of the meeting, China took a series of effective measures which played a prominent role in improving the air condition in Beijing and surrounding regions. As a result, a better quality environment emerged, which we called “APEC-Blue”. Subsequently the air condition attracts more and more attention and the atmosphere pollution become a nerve-wracking issue for a long term particularly in the North China which affects the air condition to a great extent in Beijing. Undoubtedly, aerosol pollution is a crucial problem and threat to modern society and public health.

Many fearful atmosphere pollution problems have been caused by the dramatic growth of anthropogenic emissions during the last decades in China [1,2]. The China Meteorological Agency (CMA) defined haze as weather with low visibility lower than 10 km under the situation of a relative humidity less than 90%, accompanied by the stagnant weather conditions and high air particulate matter [3–5]. High loading atmospheric pollutants can lead to haze pollution in megacities of eastern China, greatly threatening the public health [6]. In addition, dust particles or moist air masses blended with anthropogenic pollutants wandered over North China, aggravating to the serious weather and leading to widely distributed haze pollution [7]. Due to the adjustment of meteorological conditions on periodic circulation of particulate matter events in Beijing, volatile organic gas emissions mixture and nitrogen oxides from megacities transportation and sulfur dioxide from regional industrial emissions take charge for the strong secondary particulate matter formation [8].

A haze episode, causing extremely serious pollution in corresponding city clusters during November, occurred over North China and aroused the concern of the whole society. Ground-based observations describe the concentrations and temporal variations of several emission pollutants in different megacities. During the APEC summit periods, different types of haze events with different aerosol optical properties occurred over North China, leading to a wide range of pollution. However, the general characteristics of the pollution over the North China, including substantial information about its type, formation, are unclear on account of a lack of sustaining and comprehensive observations. Particularly, we have no idea about the temporal and spatial change of particles during the summit conference.

There are many effective remote sensing data to monitor aerosol properties such as ground-based observation, satellite images, *etc.* Obviously, they have some inevitable inadequacies relative to each other. Synergistic observation plays an important role in observing atmosphere conditions, which could make up for the deficiencies of the single observing method. To investigate the causes and environmental influences of the haze episodes over North China, we come up with a general overview of variations in haze episodes during the dry season using a month satellite data (November 2014) integrated with meteorological data and ground-based information. Different haze episodes processed were analyzed by accounting for ground data, satellite data and meteorological data. The different aerosol properties and meteorological conditions were also discussed in detail.

2. Experimental Section

2.1. Ground Observations and Meteorological Data

Chinese air quality on-line monitoring analysis platform is a public welfare software platform supported by many companies, research institutions and universities. From now on it has recorded PM_{2.5} and weather information of 367 cities, specifically including the AQI (Air Quality Index), particulate matter with a diameter less than 2.5 μm (PM_{2.5}) and 10 μm (PM₁₀), sulfur dioxide (SO₂), nitrogen dioxide (NO₂), ozone (O₃), carbon monoxide (CO), temperature, humidity, wind scale, wind direction and satellite cloud image. The platform, since December 2013, provides the historical data query analysis, mainly including real-time monitoring, monitoring curve, time statistics, the distribution of cities and provinces, city and global distribution, satellite cloud image, urban comparison, statistical rankings, historical analysis, association mining, *etc.*

In order to analyze the variation of anthropogenic emissions and transportation, the average values of daily concentrations of major pollutants in six urban sites were examined and compared (Figure 1). Moreover, the primary pollutants data of industrial cities, which located in the southwest of Beijing, were used to evaluate the influence of southerly industrial emissions.



Figure 1. The trajectories of air mass arriving in Zhengzhou and Jinan on 22 November.

NASA's Aerosol Robotic Network (AERONET) provides abundant aerosol characteristic parameters. Aerosol optical properties (such as aerosol optical depth (AOD), Single Scattering Albedo (SSA), *etc.*) and physical properties (such as volume size distribution with CIMEL sun photometers) were retrieved in different parts of the world [9]. SSA can be retrieved under the condition of a high aerosol loading ($AOD_{440nm} > 0.4$) with a precision of 0.03 [10]. Moreover, the size distribution was used in this paper to distinguish the fraction of fine-mode and coarse-mode particles. Level 1.5 inversion data (level 2.0 not available) of Beijing ($39.98^{\circ}N$, $116.38^{\circ}E$) site in the North China is used.

In this paper, National Centers for Environmental Prediction (NCEP) re-analysis data are used to analyze regional variations of wind fields [11]. Otherwise, meteorological sites provide essential information of meteorological conditions such as vertical variations of temperature and relative humidity (RH) in Beijing.

2.2. Satellite Data Sets

The Moderate Resolution Imaging Spectroradiometer (MODIS) on Terra and Aqua satellite retrieves many atmospheric parameters by radiance from 36 spectral bands in 0.4–14.4 μm with a swath width of 2330 km. MODIS true color images at 1 km can provide an overview of the general atmospheric conditions. Collection 6.1 MODIS AOD at 550 nm with retrieval errors within $\pm(0.05\% + 15\%)$ was used to evaluate regional aerosol loading associated with haze pollution [12,13].

The Ozone Monitoring Instrument (OMI) on board Aura satellite detects tropospheric pollutants by measuring backscattered solar radiance in 270–500 nm. Due to the significant sensibility of elevated UV-absorbing aerosols, level 2 grid data of UV (Ultraviolet) Aerosol Index (UVAI) with resolution of 0.25° were used to examine the transport of airborne dust and local fire smoke in this paper [14].

Cloud-Aerosol Lidar with Orthogonal Polarization (CALIPSO) onboard the CALIPSO satellite detects vertical structures and optical properties of aerosol and cloud layers [15]. Depolarization measurement of CALIPSO at 532 nm is especially sensitive to non-spherical dust particles [16], whose properties, such as volume depolarization ratio (VDR), are much larger than that of anthropogenic aerosols [17].

All the data above were used synergistically for research and analysis in this paper. Table 1 summarized the descriptions of satellite and ground-based data set.

Table 1. List of the data sets during the study periods.

Datasets	Parameters	Spatial Resolution	Band	Date
MODIS	true color	0.01°	0.459–0.479 nm 0.545–0.565 nm 0.620–0.670 nm	11/6, 9, 11, 19–21
	AOD	1°	550 nm	
OMI	UVAI	0.25°	Near-UV	11/6, 11, 19, 20
CALIPSO	Aerosol Subtype	2.5°	532 nm	11/8, 9, 19, 20
	Total Attenuated Backscatter	2.5°		
AERONET	Depolarization Ratio	2.5°	1064 nm/532 nm	11/6, 9, 18–21
	Attenuated Color Ratio			
NCEP	SSA			
Meteorological stations	Size distribution	2.5°	441/674/870/1020 nm	11/6, 9, 11, 19–21
	Wind fields	2.5°		11/1–23
Air condition	RH(Relative Humidity)			
	Vertical temperature PM _{2.5} , PM ₁₀ , SO ₂ , NO ₂			

3. Results and Discussion

3.1. Variations of Aerosol Pollution Particles over North China around the APEC Periods

3.1.1. Concentrations of Pollution Particles in Several Major Cities

Fine particulate matter (PM_{2.5}) can be suspended in the air for a long time and has an important effect on human health and air quality. Total suspended particulate matter (PM₁₀) refers to the solid and liquid particles floating in the air such as soot or black color particles. Nitrogen dioxide (NO₂) was mainly produced from the emission of the high-temperature combustion process, such as motor vehicles and power plants while sulfur dioxide (SO₂) was emitted from many industrial processes.

Figure 2 shows the time series of daily concentrations of principal pollutants and aerosol particles in Beijing and some other major urban regions during November 2014 when the APEC convention was held in Beijing. As exhibited in Figure 2, during the APEC meeting (from 6 to 12 November), concentrations of pollutants including PM_{2.5}, PM₁₀, SO₂ and NO₂ were clearly lower than haze days, especially in Beijing where the government measures was carried out to improve the air conditions, including traffic restriction, cutting down factories to reduce the industrial emissions and decreasing pollutants from biomass, fuel, coal burning and so on. However, compared with the abruptly higher concentration of SO₂ in Jinan (peaking at 100 µg/m³), the SO₂ in other urban regions was lower than 100 µg/m³, signifying the decline of industrial emissions. Peaks values of PM_{2.5} and PM₁₀ successively appeared in Zhengzhou, Jinan on 9 November and Shijiazhuang, Handan, Baoding and Beijing on 10 November, which clearly showing a transport process from south to north with a very slow speed due to the deduction of pollutants emission. Meanwhile, a close inspection of Figure 2 shows that PM_{2.5} concentrations of Beijing during the APEC meeting period were below 100 µg/m³, so were PM₁₀. However, the concentrations in other regions were beyond 100 µg/m³ but less than 200 µg/m³. For PM₁₀ concentrations, Beijing (around 200 µg/m³) were lower than the other regions (<100 µg/m³).

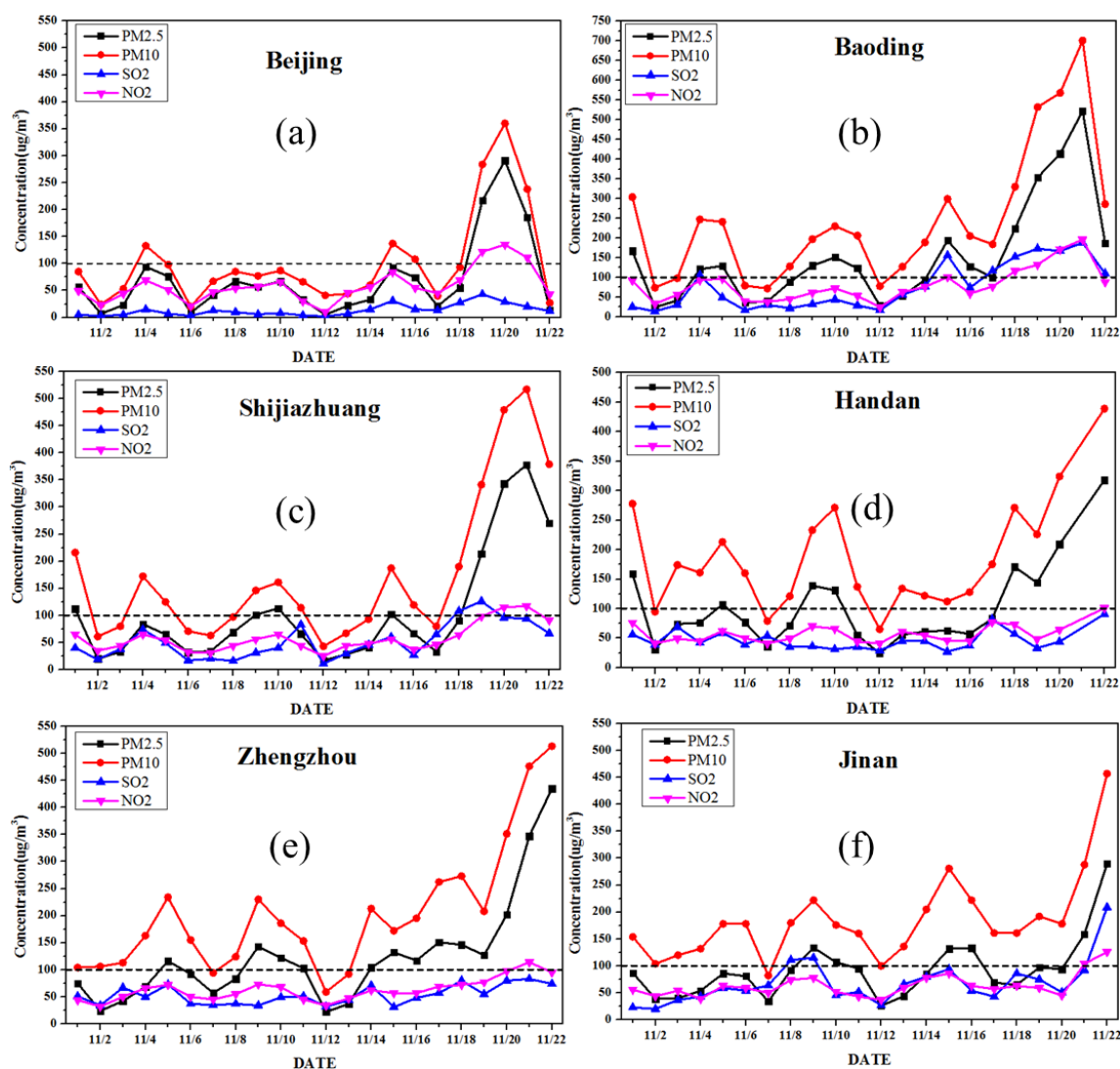


Figure 2. Daily average concentrations of PM_{2.5}, PM₁₀, SO₂ and NO₂ in several megacities ((a) Beijing; (b) Baoding; (c) Shijiazhuang; (d) Handan; (e) Zhengzhou; (f) Jinan) in North China.

After the APEC, beginning with 18 November, concentrations of gaseous pollutants of all regions turned up substantial growth with explosion. From 18 to 21 November, PM_{2.5} concentration of Beijing increased from 55 $\mu\text{g}/\text{m}^3$ to 186 $\mu\text{g}/\text{m}^3$, reaching the peak at 291 $\mu\text{g}/\text{m}^3$ on 20 November. In addition, PM₁₀ concentration rose from 93 $\mu\text{g}/\text{m}^3$ to 238 $\mu\text{g}/\text{m}^3$ with the maximum 360 $\mu\text{g}/\text{m}^3$ emerging on 20 November. However, SO₂ had no obvious change during this period when the NO₂ changed from 28 $\mu\text{g}/\text{m}^3$ to 111 $\mu\text{g}/\text{m}^3$ with the maximum value 135 $\mu\text{g}/\text{m}^3$ in 20 November. Baoding took on greatest changes among the study regions, whose peak concentrations values of PM_{2.5} and PM₁₀ increased to around 500 $\mu\text{g}/\text{m}^3$ and 700 $\mu\text{g}/\text{m}^3$ respectively at the same time. Shijiazhuang's concentrations of PM_{2.5} changed from 90 $\mu\text{g}/\text{m}^3$ to 378 $\mu\text{g}/\text{m}^3$. Even worse, PM₁₀ concentration there got a more intensively change from 190 $\mu\text{g}/\text{m}^3$ to 517 $\mu\text{g}/\text{m}^3$ where the concentrations of SO₂ and NO₂ were from 108 $\mu\text{g}/\text{m}^3$ to 94 $\mu\text{g}/\text{m}^3$ and 64 $\mu\text{g}/\text{m}^3$ to 117 $\mu\text{g}/\text{m}^3$, respectively. However, Handan was different from other cities in Hebei province, whose peak concentrations values of pollution particles appeared on 22 November same with Zhengzhou and Jinan. As one can see, although all of metropolis gaseous pollutants concentrations presented sharp upward trends relative to the APEC meeting, air condition gradually got stagnant from north to south during the four study regions. Furthermore, one can also see that the maximum of PM_{2.5} and PM₁₀ firstly appeared in Beijing in 20 November, indicating

that pollutants from local emissions and transported from surrounding regions may contribute to the haze pollution. Subsequent peaks arrived at Baoding and Shijiazhuang which is on south of Beijing on 21 November and then appeared in Handan, Jinan and Zhengzhou on 20 November. A clear transportation process of pollutants peaks from north to south turned up over North China from 19 to 22 November. Figure 1 also showed the air mass trajectories from Hebei to Zhengzhou and Jinan.

Figure 3 revealed that the huge difference of pollutants concentrations between the two periods, which indicated the significance of the measures about improving air condition and the influence of the meteorological factors. The average values of $PM_{2.5}$, PM_{10} , SO_2 and NO_2 concentrations in Beijing after APEC increased 152.15%, 119.8%, 224.13% and 88.14%, compared with those during APEC, respectively. The other five megacities increased between 43.69%–166.94%, 40.89%–146.96%, 27.14%–365.45% and 22.8%–126.82%, respectively.

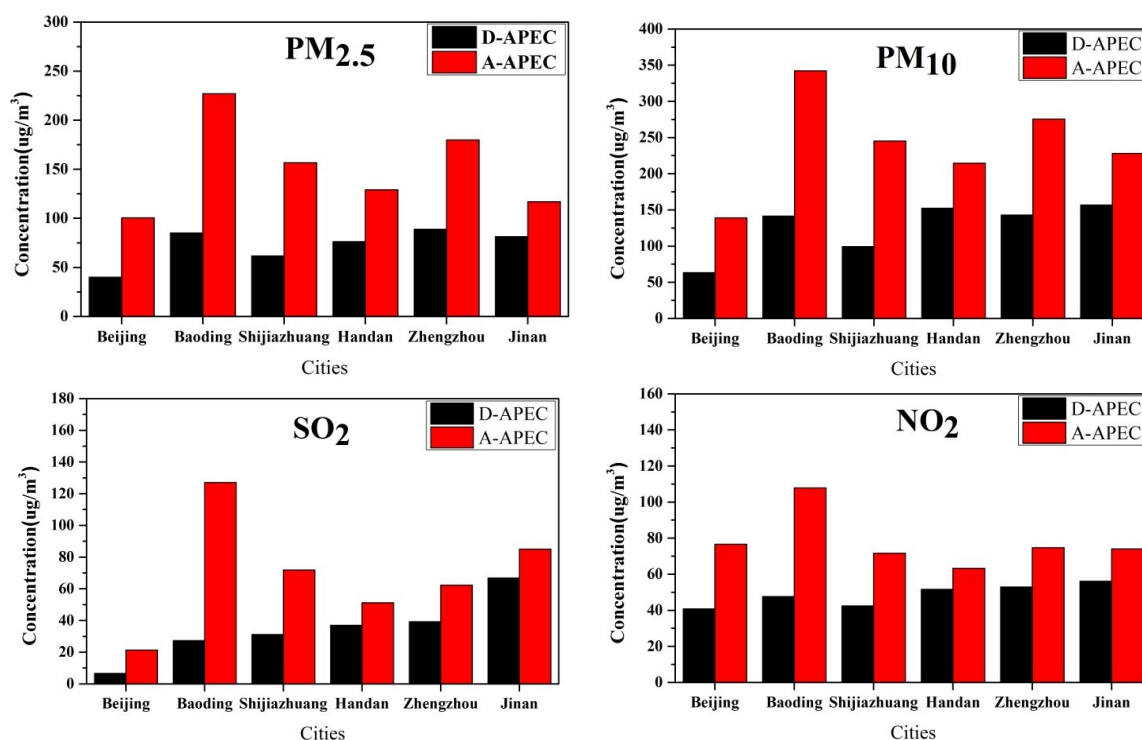


Figure 3. Average concentrations of $PM_{2.5}$, PM_{10} , SO_2 and NO_2 during (D-APEC: 6–12 November) and after(A-APEC: 13–22 November) APEC in 6 megacities.

3.1.2. Variations of Optical and Physical Properties over North China

Observations on board a satellite furnish a diverse point of haze pollution over North China from space on account of optical properties of the pollution layers. Meteorological conditions during different periods were very distinct. The MODIS true color data can depict the probable circumstance of the atmosphere over North China where widespread pollution plumes were observed over Beijing and surrounding regions. Figure 4 shows a general view of air conditions over North China. Compared with the clear air condition appeared over Beijing during APEC period and Hebei province, the aerosol loadings were still high to the south of Beijing during this period. Moreover, widespread stagnant weather occurred over North China after the meeting time. For the further studying, analysis of aerosol optical properties between the two periods was introduced in the following part.

Aerosol Optical Depth (AOD) can intuitively indicate the mass loading of particles, which may effectively give an index to the spatial distribution and variation of the aerosol particles in the atmosphere. Taking the data covering problems of North China into consideration, AOD retrieved by dark-target method was used on 6, 9, 11, 21 November and deep-blue method in 19, 20 November.

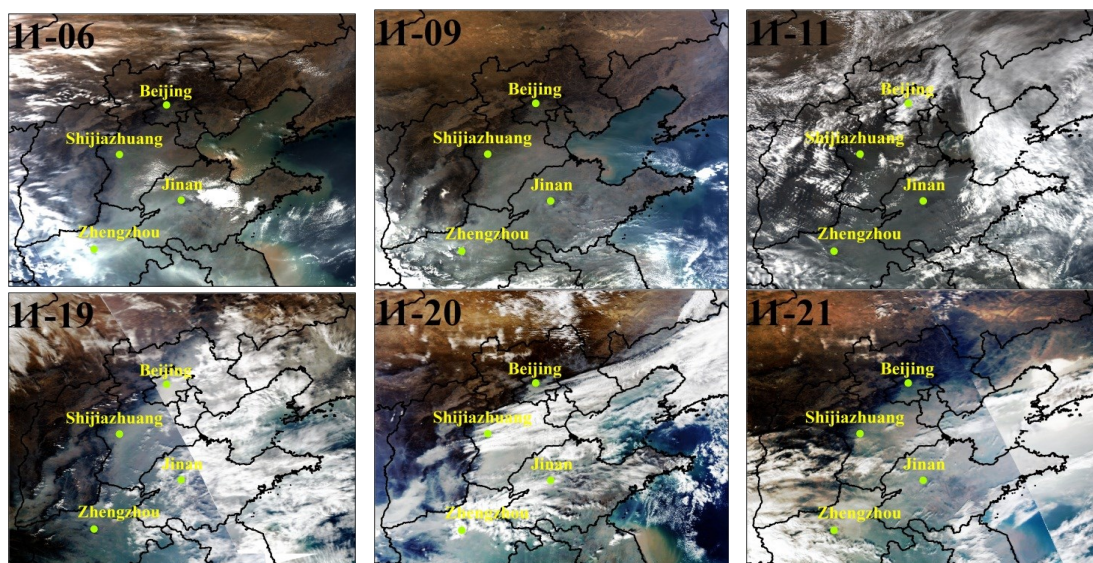


Figure 4. Aqua MODIS true color images.

During the APEC meeting, one can obviously see that even though the clear days with low AOD values (<0.2) emerged over Beijing and most of Hebei province on 6 November, a large area experienced high AOD values in the junction of Hebei, Shandong and Henan provinces, indicating that this region accumulated a great deal of anthropogenic pollutants emissions on November 9 (Figure 5). However, aerosol loadings in Beijing and its surrounding regions were at a low level during which high AOD values (>1.0) gradually spread from south (three provinces junction) to north toward Beijing but kept in the south of Hebei province.

After the meeting, air pollutants accumulated in the regions surrounding Beijing and presented an exploding and widespread growth. In the wake of the ending of the measurements the government carrying out in allusion to the summit meeting, a great deal of local pollutant was emitted and haze pollution got worse in Beijing and its surrounding regions. Subsequently aerosol loadings became increasingly higher from north to south over the study areas.

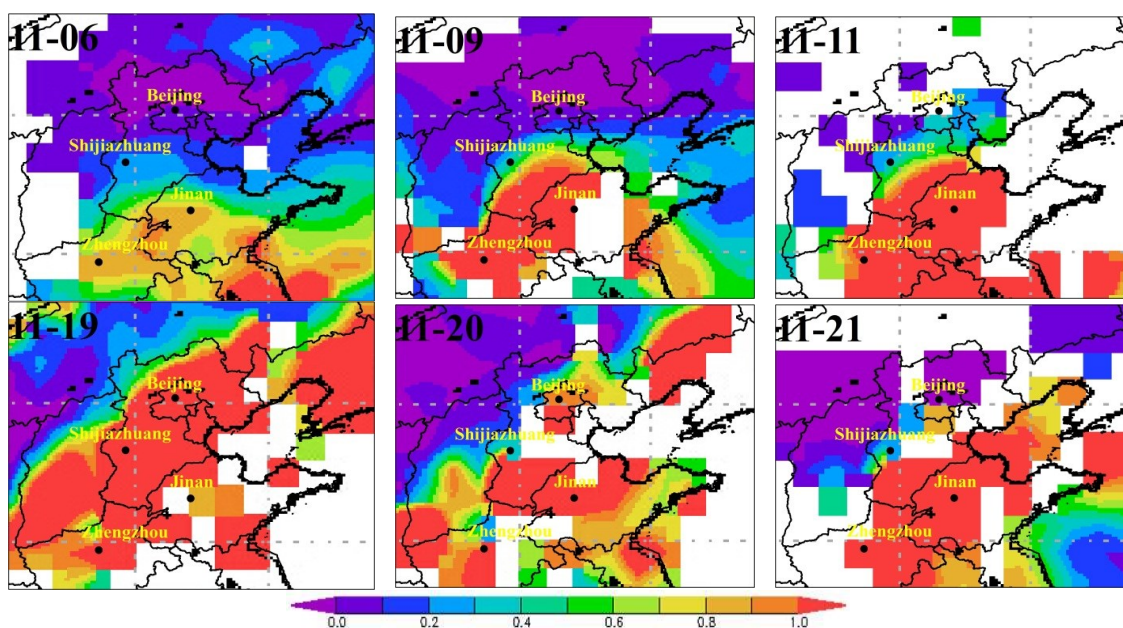


Figure 5. Aqua MODIS AOD data over North China.

UVAI values (>1.5) suggest that intensive absorption aerosols over south of Beijing regions were fierce during the APEC summit period, potentially implying the existence of dust particles or biomass burning (Figure 6). However, there were obviously UV-absorbing particles with high values (>1.5) over the junction of Hebei, Henan and Shandong, indicating the existence of the dust plumes. Meanwhile, clear weather appeared over Beijing with a low AOD (<0.2) and UVAI (<1).

After the summit, remarkable high value areas of UVAI (>2.5) turned up over North China, indicating the existence of the strong absorption aerosols such as mineral dust or smoke. Moreover, we could see that aerosol absorption properties in Beijing were more intensive with high UVAI values (>1.5). Coarse-mode aerosols with high UVAI values (>1.5) were predominant on 20 November, manifesting the increase of dust plumes in Beijing. It was concluded that western and northwestern airflows at 850 hpa were prevalent over North China during this time, which may clear the fine-mode particles over North China.

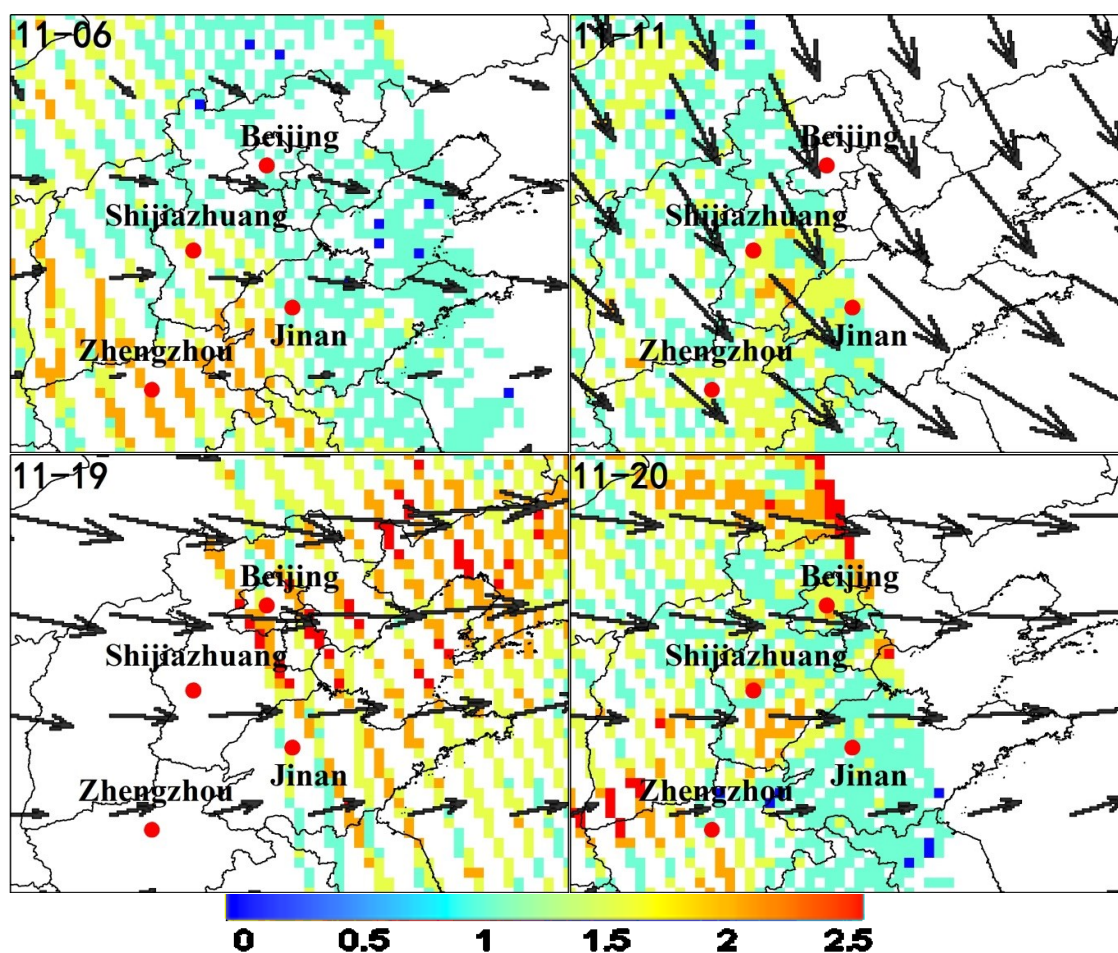


Figure 6. OMI UV Aerosol Index with 850 hpa wind fields on 6, 9, 19 and 20 November.

The single scattering albedo (SSA) is defined as the ratio of the scattering coefficient to the extinction coefficient of particles, which is the sum of the absorption and scattering coefficients. It can reflect directly the aerosol radiation forcing and reveal the relationship between scattering and absorption coefficients [18]. Moreover, aerosol volumes size distribution can suggest the particles radius under two weather conditions.

Figure 7 showed that SSA of aerosols in Beijing was at a high level ($SSA > 0.94$) during meeting periods, indicating that scattering aerosols particles played a dominant role in the clear days. Obvious difference between the two clear days was that SSA values on November 6 were higher than that on

9 November, which may indicate that high RH values coupled with low SSA values under the good air conditions. SSA values of pollution days were quite different with that of clear days. It is distinctly stated that obvious difference of SSA at 442 nm between clear days and pollution days indicated the disparate aerosol properties. SSA values at 442 nm in pollution days (<0.92) signified that absorption aerosols were predominant particles in the air while main fraction of particles in clear days were scattering aerosol ($SSA > 0.9$).

According to the distribution of particles, one can see that there was fairly a small number of aerosols during clear days. Optical volumes of fine-mode aerosols on 19 November (pollution day) increased and occupied the main fraction of aerosols, which may indicate the existence of black carbon aerosols (Figure 7). Nevertheless, abrupt haze (lasting 1–2 days) pollution occurred on 20 November and coarse-mode ($>1 \mu\text{m}$) particles accounted for the dominant fraction during pollution days, suggesting the existence of a small scale of airborne or mineral dust. Meanwhile, Fine-mode particles decreased around one time than that on 19 November.

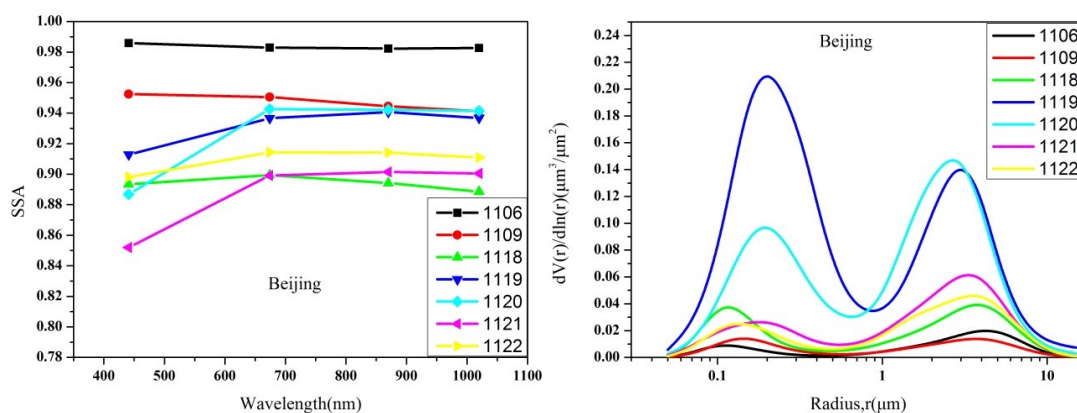


Figure 7. AERONET level 1.5 volume size distribution and single scattering albedo in Beijing site.

CALIPSO, providing the vertical observation detections of aerosol distributions, shows the optical and physical properties of the remarkable hierarchy the haze pollution layer. As we can see in Figure 8, the haze layers were at the height of the top $<3 \text{ km}$ on 8 November and 9 November. Strong extinction layers appeared within 1 km near the surface land and gradually became thicker from the south with layers $<1 \text{ km}$ to north with layers $\approx 3 \text{ km}$ over North China without extinction layers over Beijing and its surrounding regions. There existed two apparent segments over the land surface, polluted dust in the upper region and the local industrial emissions near the surface. Otherwise, the same situation appeared on 9 November, but the thickness of haze layers was thinner than that on 8 November. Backscatter extinction during these days was principally concentrated within PBL (Planetary Boundary Layer) $<3 \text{ km}$ near the land surface, indicating that dust plumes and anthropogenic emissions seem to be well mixing with each other during these periods over the land surface.

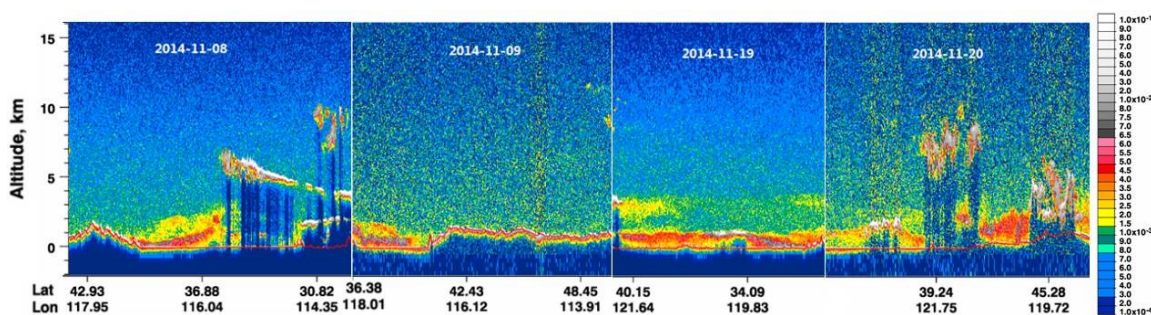


Figure 8. Cont.

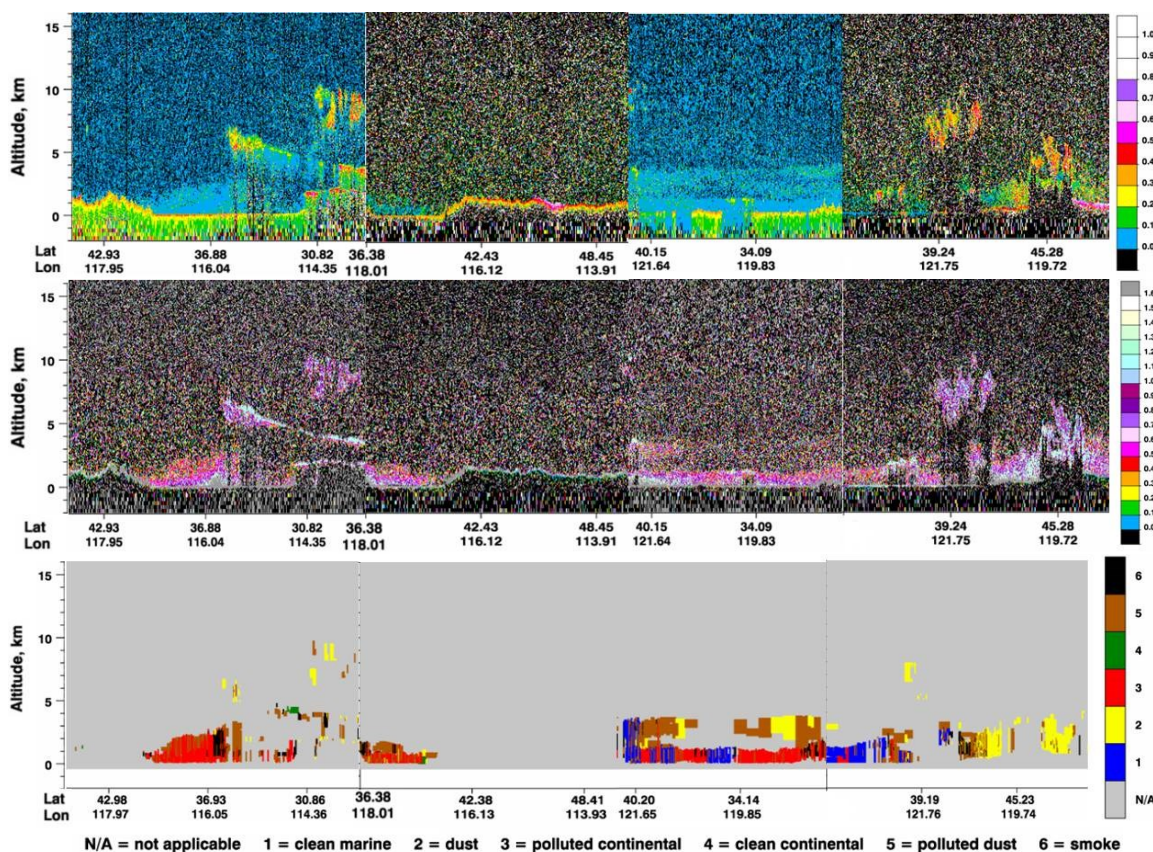


Figure 8. CALIPSO Total Backscatter at 532 nm (first floor), Depolarization Ratio (second floor), Attenuated Color Ratio (third floor) and Aerosol Subtype (fourth floor) on 6, 9, 19 and 20 November 2014.

However, after the summit meeting, on 19 November they didn't integrate well and the widespread anthropogenic pollutants were under 1 km altitude but the dust plumes were above this altitude over the circum-Bohai sea regions. Reductions of the PBL also contribute to the haze pollution [19]. It is obviously seen in Figure 7 that the heights of the PBL were at low altitudes due to the high RH which could enhance the extinction property of aerosols and strong temperature inversions may keep them at a low altitude when the stagnant weather occurred during the haze events. In addition, during the study periods we can conclude that haze pollution weather seemingly accompanied with dust plumes at a low altitude.

3.2. The Relevant Factors Leading to the Atmosphere Variations during Study Periods

Meteorological conditions during the APEC were very different. The static stability weather with low wind speed mainly appears during the period in November, which can aggravate the haze pollution and lead to the calculation of the pollutants. Prevalent temperature inversions existed in Beijing under the circumstance of stagnant weather, which were extremely strong with temperature difference reaching almost 10 °C in these days (Figure 9). Consecutive and strong temperature inversions in addition to the APEC occurred with quite low height below 500 m. Temperature inversions may appear in the situation of the fine air condition influenced by other meteorological condition.

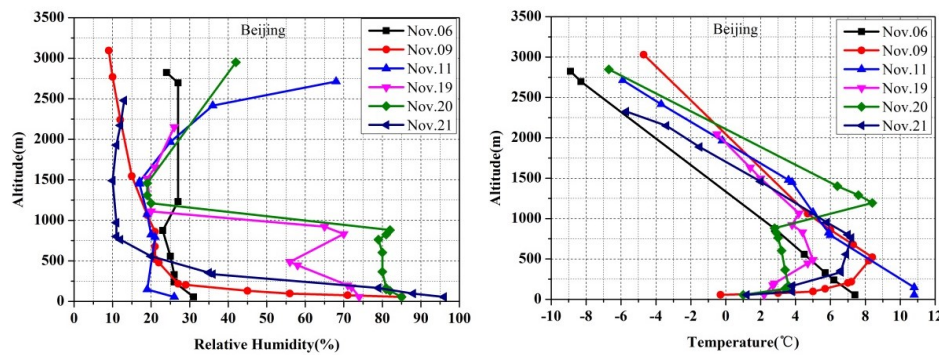


Figure 9. Vertical distributions of relative humidity and temperature in Beijing.

Another important meteorological condition factor is relative humidity (RH), which is also related to the haze days and defined as the percentage of vapor pressure in the air and the saturated vapor pressure. A good deal of hydrophilic aerosol particles, such as ammonium sulfate and ammonium nitrate, exist in Beijing [20] and the high RH could lead to not merely hygroscopic growth of particle diameters [21], but also favor aqueous phase oxidation of SO₂ and heterogeneous hydrolysis process of NO₂ [22]. These hydrophilic aerosol particles have a strong hygroscopic property, and the radius of aerosol particles can be doubled by coating with water vapor on the surface of aerosol particles under high RH value (>80%) [23]. Figure 9 shows that haze days may have a high RH among 60%~100% at a low altitude. Nevertheless, clear days could have a relative low RH values to the stagnant weather condition. However, we can see that high RH (>80%) near the land surface arose on 9 November which represented the clear day with an apparent temperature inversion layer. According to Figure 9, a strong temperature inversion may happen accompanying by a high RH weather condition whether under stagnant weather or clear days during the study period.

During the APEC meeting, airflows at 1000 hpa from north and northwest prevailed over Beijing near the land surface which prevented the pollutants transferring from the south to Beijing, indicating that meteorological conditions also played a significant role in improving air condition of Beijing.

After the meeting, airflows with low speed from the north prevailed over North China at 1000 hpa near the land surface and transported the pollutants from northern regions (Hebei province) to southern areas (Henan and Shandong province) (Figure 10). Moreover, stable weather condition with low wind speed also contributed to the accumulation of pollutants.



Figure 10. 1000 hpa wind fields over North China in study periods.

According to combining the different scale satellite data with the ground-based observations, we obtained the formation process of pollution and aerosol particle properties during the APEC periods. Not only the effective measurements played an important role in improving air conditions but also the meteorological conditions did. In addition, different scales satellite data provided the spatial and temporal variations of the aerosol particles over North China. Different transport paths of pollutants particles were influenced by meteorological conditions and anthropogenic emissions loads, which lead to the widespread atmosphere pollution over North China. Strong extinction and particles concentrated under the PBL with a low altitude (<1 km) during the whole study periods except the APEC meeting time in Beijing.

4. Conclusions

To investigate the causes and environmental influences of the haze episodes over North China, we come up with a general overview of variations in haze episodes during the dry season using a month satellite data (November 2014) integrated with meteorological data and ground-based information. In this study, we analyzed the evolution of haze pollution in Beijing around the APEC conference period with the purpose of expound the formation mechanism with combined satellite data, meteorological conditions and surface observations.

Compared the daily concentrations of pollutants observed during the APEC conference, it showed a wide difference during and after the summit meeting. During the APEC summit conference period, atmospheric pollutants gradually diffused from south to north over North China and frequent airflows from north and northwest near the land surface prevented the pollutants transferring from south of Hebei province to Beijing during the meeting period. Satellite and AERONET synergy observations show that absorption and coarse-mode aerosols were examined over North China, which may contain dust particles from northwest with airflows. Four bands of SSA in clear days always kept high values and suggested strong scattering characteristic. Nevertheless, the 442 nm band of SSA in pollution days had an obvious lower level relative to that in clear days, indicating the absorption property of aerosols. CALIPSO vertical detection shows that mixing layer with strong extinction was under PBL over the south of Beijing but with few aerosols with extinction property over Beijing region.

After the meeting days, the peak-value appeared after the conference on 20 November over Beijing, which was around three times higher than that during summit period. The extreme haze episodes were generally accompanied by strong temperature inversion and high RH near land surface, which largely contributed to the extreme haze deterioration. The pollutants were transformed from Beijing to southern part of North China with the prevalent airflows from north between 19 and 22 November. Meanwhile, the fine-mode aerosols dominated Beijing with low scatter property and strong absorption characteristic on 19 November, which might be caused by pollutants such as black carbon aerosols from local emissions. In contrast, on 20 November, coarse-mode aerosols with high UVAI (>1.5) happened over the land surface but fine-mode particles decreased a lot. This research may improve our understanding of aerosol pollution and the combining treatments of air pollution among provinces are quite necessary.

Acknowledgments: This research was supported by the National Basic Research Program of China (No: 2010CB950800), Natural Science Foundation of China (No: 41371015, 41501401, 41001207). We thank the CALIPSO, OMI and MODIS staff for the data used in our study. We also appreciate the PIs (Hui-Zheng_Che and Zheng-Qiang_Li) and their team for establishing and maintaining the Beijing AERONET sites used in this paper.

Author Contributions: Hao Chen and Tianhai Cheng conceived and supervised the research topic. Xingfa Gu and Hao Chen proposed the study methods and processed the data. Xi Wei analyzed the results and composed the paper. All authors read and approved the submitted manuscript, agree to be listed and accepted the version for publication.

Conflicts of Interest: The authors declare no conflict of interest.

References

1. Li, Z.Q.; Li, C.; Chen, H.; Tsay, S.C.; Holben, B.; Huang, J.; Li, B.; Maring, H.; Qian, Y.; Shi, G.; *et al.* East Asian Studies of Tropospheric Aerosols and their Impact on Regional Climate (EAST-AIRC): An overview. *J. Geophys. Res. Atmos.* **2011**, *116*. [CrossRef]
2. Zhang, X.Y.; Wang, Y.Q.; Niu, T.; Zhang, X.C.; Gong, S.L.; Zhang, Y.M.; Sun, J.Y. Atmospheric aerosol compositions in China: Spatial/temporal variability, chemical signature, regional haze distribution and comparisons with global aerosols. *Atmos. Chem. Phys.* **2012**, *12*, 779–799. [CrossRef]
3. Sun, Y.L.; Zhuang, G.S.; Tang, A.H.; Wang, Y.; An, Z.S. Chemical characteristics of PM_{2.5} and PM₁₀ in haze-fog episodes in Beijing. *Environ. Sci. Technol.* **2006**, *40*, 3148–3155. [CrossRef] [PubMed]
4. Tan, J.H.; Duan, J.C.; He, K.B.; Ma, Y.L.; Duan, F.K.; Chen, Y.; Fu, J. Chemical characteristics of PM_{2.5} during a typical haze episode in Guangzhou. *J. Environ. Sci.-China* **2009**, *21*, 774–781. [CrossRef]
5. Tian, S.L.; Pan, Y.P.; Liu, Z.R.; Wen, T.X.; Wang, Y.S. Size-resolved aerosol chemical analysis of extreme haze pollution events during early 2013 in urban Beijing, China. *J. Hazard. Mater.* **2014**, *279*, 452–460. [CrossRef] [PubMed]
6. Chen, Y.Y.; Ebenstein, A.; Greenstone, M.; Li, H.B. Evidence on the impact of sustained exposure to air pollution on life expectancy from China's Huai River policy. *Proc. Natl. Acad. Sci. USA* **2013**, *110*, 12936–12941. [CrossRef] [PubMed]
7. Tao, M.H.; Chen, L.F.; Su, L.; Tao, J.H. Satellite observation of regional haze pollution over the North China Plain. *J. Geophys. Res.-Atmos.* **2012**, *117*. [CrossRef]
8. Guo, S.; Hu, M.; Zamora, M.L.; Peng, J.F.; Shang, D.J.; Zheng, J.; Du, Z.; Wu, Z.; Shao, M.; Zeng, L.; *et al.* Elucidating severe urban haze formation in China. *Proc. Natl. Acad. Sci. USA* **2014**, *111*, 17373–17378. [CrossRef] [PubMed]
9. Holben, B.N.; Eck, T.F.; Slutsker, I.; Tanre, D.; Buis, J.P.; Setzer, A.; Vermote, E.; Reagan, J.A.; Kaufman, Y.J.; Nakajima, T.; *et al.* AERONET—A federated instrument network and data archive for aerosol characterization. *Remote Sens. Environ.* **1998**, *66*, 1–16. [CrossRef]
10. ODubovik, O.; Holben, B.; Eck, T.F.; Smirnov, A.; Kaufman, Y.J.; King, M.D.; Tanré, D.; Slutsker, I. Variability of absorption and optical properties of key aerosol types observed in worldwide locations. *J. Atmos. Sci.* **2002**, *59*, 590–608. [CrossRef]
11. Kalnay, E.; Kanamitsu, M.; Kistler, R.; Collins, W.; Deaven, D.; Gandin, L.; Iredell, M.; Saha, S.; White, G.; Woollen, J.; *et al.* The NCEP/NCAR 40-year reanalysis project. *Bull. Am. Meteorol. Soc.* **1996**, *77*, 437–471. [CrossRef]
12. Hsu, N.C.; Tsay, S.C.; King, M.D.; Herman, J.R. Deep blue retrievals of Asian aerosol properties during ACE-Asia. *IEEE Trans. Geosci. Remote Sens.* **2006**, *44*, 3180–3195. [CrossRef]
13. Levy, R.C.; Remer, L.A.; Kleidman, R.G.; Mattoo, S.; Ichoku, C.; Kahn, R.; Eck, T.F. Global evaluation of the Collection 5 MODIS dark-target aerosol products over land. *Atmos. Chem. Phys.* **2010**, *10*, 10399–10420. [CrossRef]
14. Torres, O.; Tanskanen, A.; Veihelmann, B.; Ahn, C.; Braak, R.; Bhartia, P.K.; Veefkind, P.; Levelt, P. Aerosols and surface UV products from Ozone Monitoring Instrument observations: An overview. *J. Geophys. Res.-Atmos.* **2007**, *112*. [CrossRef]
15. Omar, A.H.; Winker, D.M.; Kittaka, C.; Vaughan, M.A.; Liu, Z.Y.; Hu, Y.X.; Trepte, C.R.; Ferrare, R.A.; Lee, K.; Hostetler, C.A. The CALIPSO Automated Aerosol Classification and Lidar Ratio Selection Algorithm. *J. Atmos. Ocean. Technol.* **2009**, *26*, 1994–2014. [CrossRef]
16. Mielonen, T.; Arola, A.; Komppula, M.; Kukkonen, J.; Koskinen, J.; de Leeuw, G.; Lehtinen, K. Comparison of CALIOP level 2 aerosol subtypes to aerosol types derived from AERONET inversion data. *Geophys. Res. Lett.* **2009**, *36*, 18. [CrossRef]
17. Liu, Z.; Liu, D.; Huang, J.; Vaughan, M.; Uno, I.; Sugimoto, N.; Kittaka, C.; Trepte, C.; Wang, Z.; Hostetler, C.; *et al.* Airborne dust distributions over the Tibetan Plateau and surrounding areas derived from the first year of CALIPSO lidar observations. *Atmos. Chem. Phys.* **2008**, *8*, 5045–5060. [CrossRef]
18. Zhang, M.; Ma, Y.Y.; Gong, W.; Zhu, Z.M. Aerosol Optical Properties of a Haze Episode in Wuhan Based on Ground-Based and Satellite Observations. *Atmosphere* **2014**, *5*, 699–719. [CrossRef]

19. Zhang, Q.; Quan, J.N.; Tie, X.X.; Li, X.; Liu, Q.; Gao, Y.; Zhao, D. Effects of meteorology and secondary particle formation on visibility during heavy haze events in Beijing, China. *Sci. Total Environ.* **2015**, *502*, 578–584. [CrossRef] [PubMed]
20. Sun, Y.L.; Wang, Z.F.; Fu, P.Q.; Yang, T.; Jiang, Q.; Dong, H.B.; Li, J.; Jia, J. Aerosol composition, sources and processes during wintertime in Beijing, China. *Atmos. Chem. Phys.* **2013**, *13*, 4577–4592. [CrossRef]
21. Liu, X.G.; Li, J.; Qu, Y.; Han, T.; Hou, L.; Gu, J.; Chen, C.; Yang, Y.; Liu, X.; Yang, T.; *et al.* Formation and evolution mechanism of regional haze: A case study in the megacity Beijing, China. *Atmos. Chem. Phys.* **2013**, *13*, 4501–4514. [CrossRef]
22. Zhao, X.J.; Zhao, P.S.; Xu, J.; Meng, W.; Pu, W.W.; Dong, F.; He, D.; Shi, Q.F. Analysis of a winter regional haze event and its formation mechanism in the North China Plain. *Atmos. Chem. Phys.* **2013**, *13*, 5685–5696. [CrossRef]
23. Liu, J.J.; Zheng, Y.F.; Li, Z.Q.; Flynn, C.; Welton, E.J.; Cribb, M. Transport, vertical structure and radiative properties of dust events in southeast China determined from ground and space sensors. *Atmos. Environ.* **2011**, *45*, 6469–6480. [CrossRef]



© 2015 by the authors; licensee MDPI, Basel, Switzerland. This article is an open access article distributed under the terms and conditions of the Creative Commons by Attribution (CC-BY) license (<http://creativecommons.org/licenses/by/4.0/>).